**Tuijin Jishu/Journal of Propulsion Technology**
**ISSN: 1001-4055**
**Vol. 44 No. 4 (2023)**

# Numerical study on effective thermal conductivity of polymer composites with randomly distributed multi-fillers

**[1],*Ich Long Ngo, [1]Van Tuyen Vu**

*[1] School of Mechanical Engineering, Hanoi University of Science and Technology,*

*No. 01, Dai Co Viet, Hai Ba Trung, Hanoi, Vietnam*

***Abstract*—**This paper presents a numerical investigation of the effective thermal conductivity (hereafter, ETC) of polymer composites with randomly distributed multi-fillers. A finite element method combined with a user-defined code was proposed to predict the ETC under various effects. Consequently, the polymer composite structure was well generated for single, hybrid, and particularly triple fillers. The numerical results were thoroughly validated by comparing them with the prediction models, as well as numerical and experimental results in the literature. The highly complex behavior of the ETC in terms of effective parameters is first explored. The ETC of the triple-filled polymer composite improves compared with single and hybrid fillers only if the different filler's TCs are used. Otherwise, the ETC slightly reduces if the filler's TCs have the same value. The results obtained are very useful in understanding the complex behavior of the ETC of polymer composites with multiple fillers.

**Index Terms—***Finite element method, Polymer composite, Thermal conductivity, Multiple filler.*

## I. Introduction

Enhancing the material's thermal conductivity (hereafter, TC) is desirable for many technological applications, such as 5G communication equipment, electronic packages, energy transmissions, thermal management of electronic and photonic devices, heat exchangers, energy converters, building insulators, and related fields, particularly where high operating temperature is required [1]-[8]. Additionally, the TC enhancement becomes particularly important in synthesizing advanced polymer composites. Utilizing highly thermally conductive fillers, such as metals, carbon-based materials, and ceramics, represents a promising approach for enhancing the TC of pure polymers [9]-[11]. Many researchers reported that the TC is enhanced by adding fillers with high TC. For example, the PDMS composite's TC is up to 2.73 $Wm^{-1}K^{-1}$ with 20 wt% CF filler loading [12]. The literature has proved that the composite material's TC can improve significantly. Notably, planar graphite fillers have been reported to achieve remarkably high TC values, reaching 3000 $Wm^{-1}K^{-1}$ [13]. Thermally conductive fillers into polymer composite matrix have many potentials owing to their facile process, low corrosion, lightweight, and low manufacturing cost, etc. [14]-[17].

During the past few decades, a considerable number of research works has been done to enhance the TC under various factors of filler network, including the filler types, sizes (from mesoscale to nanoscale), and filler shapes (e.g., sphere, hollow sphere, platelet, tube, or fiber). Based on the number of fillers used, they can be classified into two main types: mono-fillers (or single fillers) and multi-fillers (e.g., hybrid, triple, etc.). Firstly, single fillers were used. Previous studies reported that the filler's properties and characteristics greatly affected the TC, such as the volume fraction of the filler (hereafter, VF) [18], the filler TC, the filler's size and shape, organization and positioning in the matrix, the agglomerated state of fillers, and interfacial thermal resistance on the incorporation of the matrix material [19]-[24]. Core-shell nanoparticles have also received much interest in recent years [25]-[27]. In

**Tuijin Jishu/Journal of Propulsion Technology**
**ISSN: 1001-4055**
**Vol. 44 No. 4 (2023)**

addition, hybrid fillers (combining two fillers with the same or different properties, shapes, and sizes) have been widely acknowledged as one of the promising candidates for enhancing the polymer composite's TC. This is because of the essential formation of synergistic impact on the TC of hybrid-filled polymer composites [28]. Indeed, many studies indicated that higher TC can be obtained using the hybrid fillers at a certain condition, and it is higher than the use of single fillers for the same VF [29]-[30]. Furthermore, Sanada et al. [31] reported that adding nanofillers into the polymer matrix containing the micro-ones can improve the TC of polymer composites.

Moreover, multi-fillers have attracted much attention in recent years, although this filler type is complex. As expected, triple fillers can enhance the TC of polymer composites. This type of filler can form large thermally conductive chains, and the particle package density can be improved. Additionally, triple fillers may help to reduce the overall filler loading [32]. Some worse cases, like brittleness and agglomeration, can degrade the matrix polymer's mechanical and processing properties and reduce the total product cost rather than using high filler loadings [32]. As reported by Gao et al. [33], a very high TC of epoxy composites filled with aluminum oxide, aluminum nitride, and graphene was obtained. The maximum increase of TC was up to 185% compared to that of pure epoxy, and it was also higher than that of both single and hybrid fillers. To our best knowledge, no numerical research considers the TC enhancement for polymer composites with a variety of heterogeneous fillers.

This research aims to examine the effective thermal conductivity (hereafter, ETC) of polymer composites using a variety of heterogeneous fillers. The finite element method combined with user-defined code in MATLAB was used for predicting the ETC of such polymer composites. The effects of particle distribution and other important parameters are examined extensively. In addition, an analysis and discussion of the thermal characteristics exhibited by the ETC as influenced by the diverse effects of multi-fillers.

## II. NUMERICAL METHODOLOGY

Fig. 1 illustrates a schematic representation of the numerical model used in this study. The boundary conditions (hereafter, BC) are also provided to simulate thermal flow through a polymer composite structure. The unit cell serves as an appropriate control volume due to the extensive dispersion of particles throughout the matrix. Firstly, the user-defined code generated a geometrical model of the unit cell in MATLAB. In this regard, particle-1 (yellow) was first distributed randomly and iteratively, then particle-2 (green) was distributed. At this point, particle-2 does not contact both itself and particle-1. This process is also applied to particle 3 (red). These particles are assumed to exist in isolation, with a random distribution within the matrix material. This is reasonable when the volume fraction (VF) of fillers is small (e.g., less than 0.1) to prevent brittleness and agglomeration that reduces the mechanical and processing properties of the polymer, as mentioned in the Introduction section. Finally, the geometrical model was tested and then imported into COMSOL through a module of Livelink for MATLAB. The present study aims to incorporate the impact of anisotropic particle distribution, which closely mimics the distribution observed in the experimental procedure. Additionally, the TCs of all spherical particles ($k_{p1}$, $k_{p2}$, $k_{p3}$) and matrix material ($k_m$) are assumed to be constant [30]-[34].

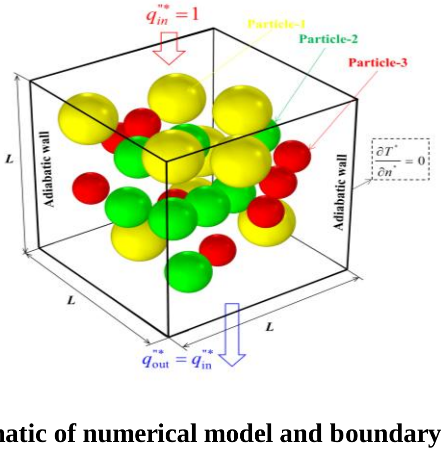


**Fig. 1. Schematic of numerical model and boundary conditions.**

**Tuijin Jishu/Journal of Propulsion Technology**
**ISSN: 1001-4055**
**Vol. 44 No. 4 (2023)**

---

Laplace equations explain how heat is transferred in a composite structure. This obeys Fourier's law with no heat generation. Consequently, the general form of these equations applied for all domains is shown in Eq. (1).

$$\partial/\partial x\left(k_{\mathrm{i}}\,\partial T_{\mathrm{i}}/\partial x\right)+\partial/\partial y\left(k_{\mathrm{i}}\,\partial T_{\mathrm{i}}/\partial y\right) +\partial/\partial z\left(k_{\mathrm{i}}\,\partial T_{\mathrm{i}}/\partial z\right)=0 \quad \mathrm{i}\ = 1, 2, 3, \mathrm{m} \tag{1}$$

The subscripts "1", "2", "3" and "m" denote the particle-1, particle-2, particle-3, and matrix, respectively. Eq. (1) can be converted into a dimensionless form using the variables shown in Eq. (2).

$$x^{*}=x/L;\ y^{*}=y/L;\ z^{*}=z/L;\ k_{\mathrm{i}}^{*}=k_{\mathrm{i}}/k_{\mathrm{m}};\ T_{\mathrm{i}}^{*}=\left(T_{\mathrm{i}}-T_{\mathrm{out}}\right)/\left(q_{\mathrm{in}}^{''}L/k_{\mathrm{m}}\right) \tag{2}$$

where the characteristic length, denoted as $L$, represents the dimension of a unit cell, as illustrated in Fig. 1. It is important to note that the heat flux was specifically defined. The surface on the top of the unit cell is the inlet to establish the characteristic temperature. This choice is motivated by the fact that the heat flux BC should be employed in this model. It is worth mentioning that this BC is commonly utilized in most experimental setups for TC measurements. Consequently, it is anticipated that the results obtained based on this BC exhibit a higher accuracy level than those obtained using the isothermal BC, as mentioned in previous studies. As a result, the Eq. (1) becomes the Eq. (3) for non-dimensional form:

$$\partial/\partial x^{*}\left(k_{\mathrm{i}}^{*}\,\partial T_{\mathrm{i}}^{*}/\partial x^{*}\right)+\partial/\partial y^{*}\left(k_{\mathrm{i}}^{*}\,\partial T_{\mathrm{i}}^{*}/\partial y^{*}\right) +\partial/\partial z^{*}\left(k_{\mathrm{i}}^{*}\,\partial T_{\mathrm{i}}^{*}/\partial z^{*}\right)=0 \quad \mathrm{i}\ = 1, 2, 3, \mathrm{m} \tag{3}$$

The important non-dimensional parameters in this research are TC ratios between the particles and the matrix $\kappa_1$, $\kappa_2$, $\kappa_3$ and the particle VFs $\phi_1$, $\phi_2$, $\phi_3$. These parameters are defined in Eq. (4) as:

$$\kappa_1=k_1/k_{\mathrm{m}};\ \kappa_2=k_2/k_{\mathrm{m}};\ \kappa_3=k_3/k_{\mathrm{m}};\ \phi_1=N_1V_1/V_{\mathrm{cell}};\ \phi_2=N_2V_2/V_{\mathrm{cell}};\ \phi_3=N_3V_3/V_{\mathrm{cell}} \tag{4}$$

where $N_1$, $N_2$ and $N_3$ represent the number of particle-1, particle-2, and particle-3 per unit cell, respectively, $V_1$, $V_2$, $V_3$, and $V_{\mathrm{cell}}$ stands for the volumes of particle-1, particle-2, particle-3, and unit cell. Based on the Fourier's equation, the ETC of polymer composite can be determined by Eq. (5):

$$k_{\mathrm{eff}}=-Q/\left[L\left(T_{\mathrm{in}}-T_{\mathrm{out}}\right)\right] \tag{5}$$

In this equation, $Q$ represents the total heat transfer rate. Eq. (5) becomes Eq. (6) in the dimensionless form, where the average temperature ($\bar{T}_{\mathrm{in}}^{*}$) is determined at the top surface.

$$k_{\mathrm{eff}}^{*}=k_{\mathrm{eff}}/k_{\mathrm{m}}=1/\bar{T}_{\mathrm{in}}^{*} \tag{6}$$

## III. Results and Discussions

### A. *Single filler*

**Table I. Some structures of the polymer composite with single fillers.**

| $\phi$=0.15, $\kappa$=2250 | | |
|---|---|---|
| $N$ = 3 | $N$ = 9 | $N$ = 30 |
| 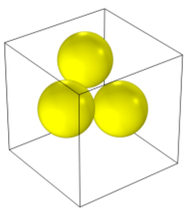 | 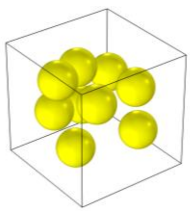 | 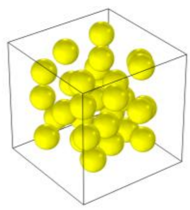 |

| | | |
|---|---|---|
| $k_{eff}$* = 1.59<br>SA = 1.969 | $k_{eff}$* = 1.55<br>SA = 2.839 | $k_{eff}$* = 1.55<br>SA = 4.242 |

Table I shows the effects of the number of single fillers ($N$) with VFs of single filler at 0.15 and the TC equal to 2250. Three cases of $N$ are the small value ($N$=3), the medium ($N$=9), and the large value ($N$=30). Based on this table, it was found that the polymer composite structure was well generated for single fillers with various $N$ values. Additionally, the ETC slightly decreases with decreasing the particle size or increasing the number of particles. Notably, the surface area (hereafter, SA) increases with increasing the number of particles while keeping the VF constant.

The numerical model provided in Section II was first validated by comparing it with a well-known model developed by Nan et al. [35] for single filers. The dimensional form of Nan's model applied for single spherical particles is shown in Eq. (7) as follows:

$$k_{\mathrm{eff}}^{*} = 1 + \frac{3\phi(\kappa - 1)}{2 + \phi + \kappa(1 - \phi)} \qquad (7)$$

Fig. 2 shows the comparison between the ETCs from the present work and those by Nan's model [35] with VFs ranging from 0 to 0.3 for two cases of TC ratios, $\kappa$ = 3 and $\kappa$ = 30. Consequently, the numerical results match those obtained by Nan's model, particularly when VFs are less than 0.25. There is a minor deviation at the high VF because of some factors, such as the effects of particle distribution and particle size.

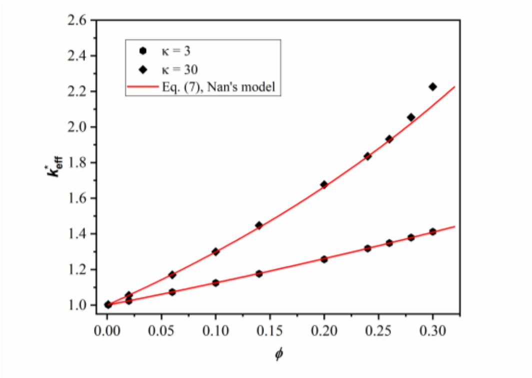


**Fig. 2. Comparison between the ETCs from present work and those by Nan's model [35], Eq. (8) for two TC ratios, $\kappa$ = 3 and $\kappa$ = 30**

Fig. 3 shows the ETCs as a function of VF under the effects of random particle distribution for three values of $N$. The VF ranges from 0 to 0.25. Here, fifty random cases are considered for each VF. This figure indicated that the effect of particle distribution becomes large at the high VFs. Moreover, the ETC variation gradually shrinks at the smaller particle size or larger number of particles (e.g., $N$=30). It implies that more testing cases should be performed to obtain the high ETC when the large-size particles are randomly distributed in the polymer matrix.

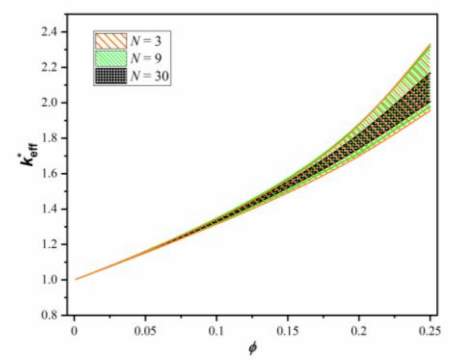


**Fig. 3. ETCs as a function of volume fraction with effects of random particle distribution. $\kappa = 800$**

*B. Hybrid fillers*

Table II shows the effects of the number of hybrid fillers with three cases, small, medium, and large number of particles, in the same operating condition. Total VF $\phi_s$ ($\phi_s = \phi_1 + \phi_2$), VF ratio $\phi_d = \phi_2/\phi_1$, total TC $\kappa_s = \kappa_1 + \kappa_2$, and the TC ratio $\kappa_d = \kappa_2/\kappa_1$ are used to examine the mutual effect of hybrid fillers. In this table, particles 2 (green) are added compared with a single filler. The SA is calculated for both particle 1 and particle 2, respectively. As a result, the polymer composite structure was well generated for hybrid fillers with various $N$ values. Additionally, the ETC varies slightly regardless of increasing the SA or the particle size.

**Table II. Some structures of the polymer composite with hybrid fillers.**

| $\phi_s = 0.15$, $\phi_d = 0.5$, $\kappa_s = 2250$, $\kappa_d = 4$ | | |
|---|---|---|
| $N_1 = N_2 = 3$ 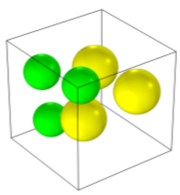 | $N_1 = N_2 = 9$ 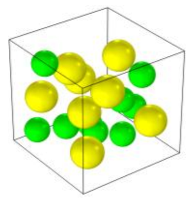 | $N_1 = N_2 = 30$ 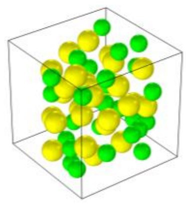 |
| $k_{eff}^* = 1.54$<br>SA = 2.45 | $k_{eff}^* = 1.55$<br>SA = 3.53 | $k_{eff}^* = 1.54$<br>SA = 5.28 |

As reported in the literature, the Hashin-Shtrikman (HS) model can predict the TC of composites with randomly distributed particles [36]-[37]. Moreover, a modified HS model is proposed by Ngo et al. [38], which is shown by Eq. (8). In this model, correction factor λ varies from 0.5 to 5 depending on relevant effects, such as particle distribution, particle size, and even the TCR.

$$k_{eff}^* = \frac{1 + 2\lambda\left(\frac{\kappa_1 - 1}{\kappa_1 + 2}\phi_1 + \frac{\kappa_2 - 1}{\kappa_2 + 2}\phi_2\right)}{1 - \lambda\left(\frac{\kappa_1 - 1}{\kappa_1 + 2}\phi_1 + \frac{\kappa_2 - 1}{\kappa_2 + 2}\phi_2\right)} \quad \text{where } \lambda = 0.5 \sim 5 \qquad (8)$$

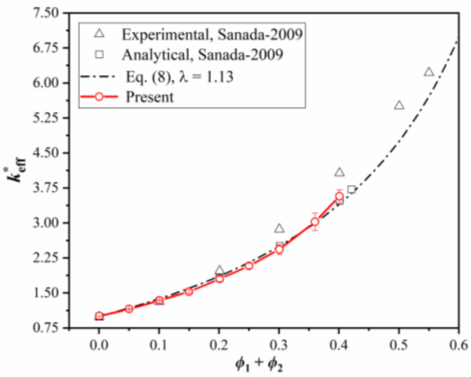


**Fig. 4. Validation with experimental and analytical results obtained by Sanada et al. [31], $\phi_1$=8$\phi_2$, $\kappa_1$=$\kappa_2$=173.1, error bars show an SD of ETC due to particle distribution.**

The results obtained by Eq. (8) were compared with those from the present work, as shown in Fig. 4. Moreover, the experimental and analytical results obtained by Sanada et al. [31] were also included in this figure with the VF ranging from 0 to 0.3. It was found that the numerical results from the present study are in very good agreement with those obtained by the modified HS model and Sanada et al. [31] in the entire considered ranges. Particularly, the deviation of the ETC compared to the analytical results obtained by Sanada et al. [31] is less than 3%. It implied that the numerical results were well-validated.

Fig. 5 shows the effects of random particle distribution for various values of *N*. Fifty random cases are also considered for each VF to examine the effects of particle distribution. Consequently, the behavior of the ETC resembles that obtained for a single filler mentioned in Section A. Indeed, the effect of particle distribution becomes large at the high VFs, and the ETC variation gradually shrinks at the smaller particle size. However, the ETC possibly lifts to the high VF range. This is because the synergic effect exists, and the maximum particle packing can be improved for hybrid fillers compared to single fillers.

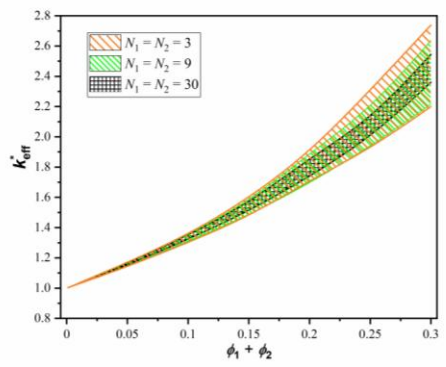


**Fig. 5. ETC as a function of volume fraction with effects of random particle distribution with $\phi_1$=10$\phi_2$, $\kappa_1$=160, $\kappa_2$=640, $\kappa_s$=800.**

*C. Triple fillers*

The user-defined code in MATLAB was also developed for triple-filled polymer composite. Like hybrid filler, the following parameter were defined: $\phi_s$ ($\phi_s$=$\phi_1$+$\phi_2$+$\phi_3$), $\phi_{d1} = \phi_2/\phi_1$, $\phi_{d2} = \phi_3/\phi_1$, total TC $\kappa_s$=$\kappa_1$+$\kappa_2$+$\kappa_3$, and the ETC ratio $\kappa_{d1} = \kappa_2/\kappa_1$, $\kappa_{d2} = \kappa_3/\kappa_1$. Again, Table III also indicated that the polymer composite structure was well generated for triple fillers with various operating conditions. Additionally, the ETC slightly increases with increasing the number of particles. These results are consistent with those obtained for single and hybrid fillers.

**Table III. Some structures of the polymer composite with triple fillers.**

| $\phi_s$=0.15, $\phi_{d1}$=0.5, $\phi_{d1}$=2, $\kappa_s$=2250, $\kappa_{d1}$ = 0.25, $\kappa_{d2}$ = 0.5 | | |
|---|---|---|
| $N_1$=$N_2$=$N_3$=3 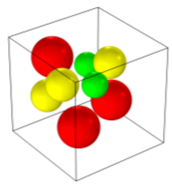 | $N_1$=$N_2$=$N_3$=9 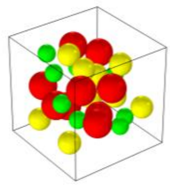 | $N_1$=$N_2$=30 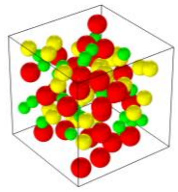 |
| $k_{eff}$* = 1.54<br>SA = 1.97 | $k_{eff}$* = 1.55<br>SA = 2.84 | $k_{eff}$* = 1.54<br>SA = 4.24 |

To effectively predict the TC of polymer composites with triple fillers, prediction models can be developed. First, the Lewis-Nielsen model [39] was proposed, as shown in Eq. (9), but for triple fillers. For the spherical fillers, $B_i$ equals 1.5, and the maximum packing fraction of particles, $\phi_{m,i}$ is 0.637 [39]-[41].

$$k_{\text{eff}}^{*} = \left[1+\sum_{i=1}^{3} B_i C_i \phi_i\right] \Big/ \left[1-\sum_{i=1}^{3} C_i D_i \phi_i\right] \quad \text{where} \begin{cases} C_i = [\kappa_i - 1]/[\kappa_i + A]_i ;\ D_i = 1 + \left[\left(1-\phi_{m,i}\right)/\phi_{m,i}^2\right]\phi_i \\ B_i \text{ and } \phi_{m,i} \text{ depend on filler shape and orientation} \end{cases} \tag{9}$$

Second, a model originated from the Hashin-Shtrikman model [36]-[37] was also developed for triple fillers, as given by Eq. (10).

$$k_{\text{eff}}^{*} = \left(1+2\sum_{i=1}^{3} E_i \phi_i\right) \Big/ \left(1-\sum_{i=1}^{3} E_i \phi_i\right) \text{ where } E_i = \frac{\kappa_i - 1}{\kappa_i + 2} \tag{10}$$

Finally, a modified HS model proposed by Ngo et al. [38] was considered, as shown in Eq. (11).

$$k_{\text{eff}}^{*} = \frac{1+2\lambda\left(\dfrac{\kappa_1-1}{\kappa_1+2}\phi_1 + \dfrac{\kappa_2-1}{\kappa_2+2}\phi_2 + \dfrac{\kappa_3-1}{\kappa_3+2}\phi_3\right)}{1-\lambda\left(\dfrac{\kappa_1-1}{\kappa_1+2}\phi_1 + \dfrac{\kappa_2-1}{\kappa_2+2}\phi_2 + \dfrac{\kappa_3-1}{\kappa_3+2}\phi_3\right)} \tag{11}$$

where $\lambda = 0.5 \sim 5$

All models mentioned above satisfy the following important properties from a physical viewpoint: (i) the role of three particles is equivalent, and (ii) the ETC always equals unity if the VF of three particles is zero, regardless of the TC ratios, or if TC ratios of fillers equal unity regardless of their VFs. It implies that predicting the ETC of polymer composite with triple fillers is feasible under a given operating condition.

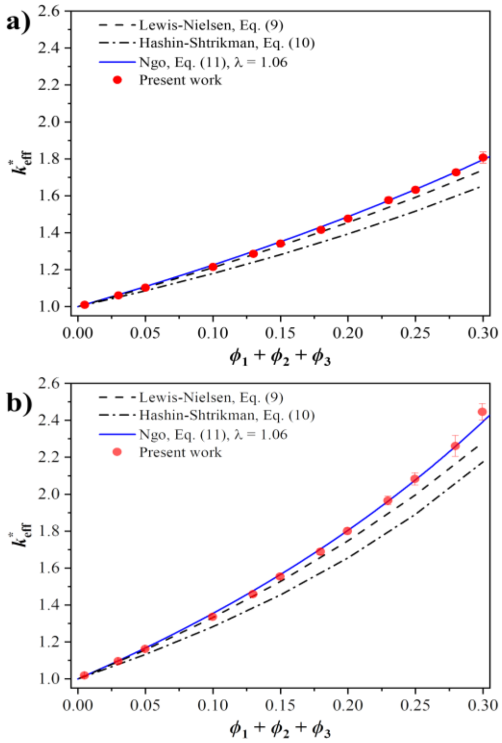


**Fig. 6. ETC of hybrid filler polymer composites obtained from various models and present work, (a) $\phi_1$=$\phi_2$=$\phi_3$, $\kappa_1$=1, and $\kappa_2$=150, $\kappa_3$=1020, (b) $\phi_1$=2$\phi_2$=4$\phi_3$, $\kappa_1$=1020, $\kappa_2$=1600, and $\kappa_3$=2250, $N_1$=10, $N_2$=15, and $N_3$=25. Error bars show the standard deviation of ETC due to particle distribution.**

Fig. 6 shows the comparison between the ETC from the present work and the results obtained by the prediction models (from Eq. (9) to Eq. (11)). Fig. 6a shows the lower TC with $\phi_1$=$\phi_2$=$\phi_3$ and Fig. 6b shows the higher TC with operating condition $\phi_1$=2$\phi_2$=4$\phi_3$ (Fig. 6b). Notably, it can be assumed $\phi_1$> $\phi_2$ > $\phi_3$ since the role of fillers in the composite structure is equivalent. Consequently, it was found from Fig. 6 that the numerical results are in very good agreement with those obtained by Modified Lewis-Nielsen's HS model, particularly the modified HS model proposed by Ngo et al. [38].

**Table IV. Temperature contour on two mid planes for the same VF of 0.12, $N_1$=$N_2$=$N_3$=3**

| **VF** | **Plane** **$x^*$ = 0.5** | **Plane** **$z^*$ = 0.5** | **Quantities** |
|---|---|---|---|
| | $\kappa_1$=10, $\kappa_2$=190, and $\kappa_3$=1000 | | |
| $\phi$=0.12 | 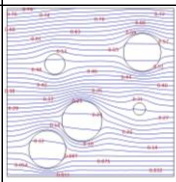 | 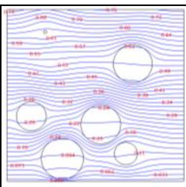 | (a) *Single filler* $k_{eff}$*=1.31 SA= 2.89 |
| $\phi_1$=0.04 $\phi_2$=0.08 | 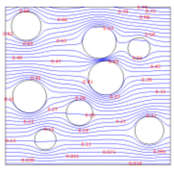 | 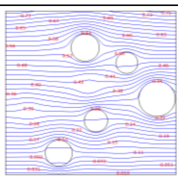 | **(b)** *Hybrid filler* $k_{eff}^*$ = 1.38 SA=3.60 |

| | | | |
|---|---|---|---|
| $\phi_1$=0.01<br>$\phi_2$=0.04<br>$\phi_3$=0.07 | 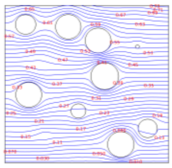 | 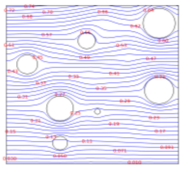 | **(c)**<br>*Triple filler*<br>$k_{eff}^*$ = 1.41<br>SA= 5.62 |
| | $\kappa_1$=$\kappa_2$= $\kappa_3$=400 | | |
| $\phi$=0.12 | 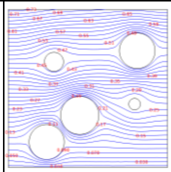 | 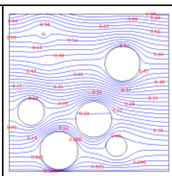 | **(d)**<br>*Single filler*<br>$k_{eff}^*$ = 1.45<br>SA= 2.89 |
| $\phi_1$=0.04<br>$\phi_2$=0.08 | 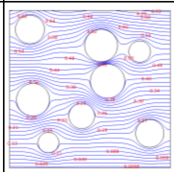 | 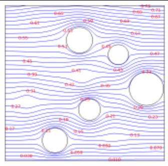 | **(e)**<br>*Hybrid filler*<br>$k_{eff}^*$ = 1.42<br>SA= 3.60 |
| $\phi_1$=0.01<br>$\phi_2$=0.04<br>$\phi_3$=0.07 | 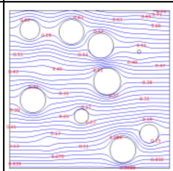 | 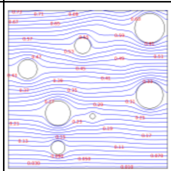 | **(f)**<br>*Triple filler*<br>$k_{eff}^*$ = 1.42<br>SA= 5.62 |

**Fig. 7 shows the variation of ETC under the effects of particle distribution for two particular cases of VF ratio, $\phi_{d1}$=$\phi_{d2}$=0.1 (Fig. 7a) and $\phi_{d1}$=$\phi_{d2}$=1.0 (Fig. 7b). The yellow, blue, and red surfaces represent the minimum, mean and maximum ETC, respectively. The ETC variation depends on both $\kappa_{d1}$ and $\kappa_{d2}$. It was found from Fig. 7 that the highly complex behavior of the ETC in terms of effective parameters is first explored. Indeed, the mountain shape of ETC forms and depends on various parameters, including $\kappa_{d1}$, $\kappa_{d2}$, $\phi_{d1}$, and $\phi_{d2}$. The extreme point of the ETC is ETC obtained when two TC ratios are less than 1.0 (Fig. 7a); however, the extreme point ETC point moves and is close to the bar line ($\kappa_{d1}$ = $\kappa_{d2}$ = 1) (Fig. 7b).**

Table IV shows the temperature iso-contour on two mid planes $x^*$ =0.5 and $z^*$ =0.5 for total VFs of 0.12 and the same number of particles for three cases: single, hybrid, and triple fillers. For the different TCs ($\kappa_1$=10, $\kappa_2$=190, and $\kappa_3$=1000), the ETC increases from 1.31 (single filler) to 1.41 (triple fillers). On the other hand, the ETC slightly decreases from 1.45 (single filler) to 1.42 (triple fillers) for the same TC case. In summary, the ETC of the triple-filled polymer composite improves compared with single and hybrid fillers only if the different filler's TCs are used. Otherwise, the ETC slightly reduces if the filler's TCs have the same value.

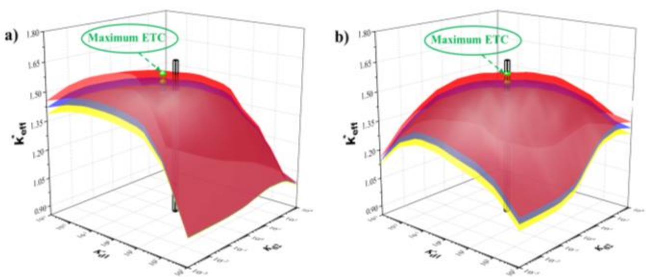


**Fig. 7. Effects of particle distribution on the maximum ETC, (a) $\phi_{d1}$ = $\phi_{d2}$ = 0.1 and (b) $\phi_{d1}$ = $\phi_{d2}$ = 1.0, $\phi_s$=0.15, $\kappa_s$ =800, and $N_1$ = $N_2$ = $N_3$ = 5 were used for all cases.**

## IV. Conclusion

The TC of multi-filler polymer composites has been studied numerically and analytically. Geometrical models with randomly distributed mono-fillers (single filler) and multi-fillers (hybrid and triple fillers) were built by The Livelink for MATLAB with COMSOL. Then, the ETC was predicted accurately and effectively by the finite element method. The numerical results were thoroughly validated by comparing them with well-known models, other numerical results, and experimental results for single filler, hybrid, and triple fillers. The ETC is examined under various effects. The polymer composite structure was well generated for single, hybrid, and particularly triple fillers. Furthermore, the random particle distribution affects the ETC significantly, particularly at high total VFs where the ETC variation is extended. Additionally, the highly complex behavior of the ETC in terms of effective parameters is first explored. The maximum ETC depends on depends on various parameters, including $\kappa_{d1}$, $\kappa_{d2}$, $\phi_{d1}$, and $\phi_{d2}$. The ETC of the triple-filled polymer composite improves compared with single and hybrid fillers only if the different filler's TCs are used. Otherwise, the ETC slightly reduces if the filler's TCs have the same value. The results obtained can be used to enhance the ETC of polymer composites with multiple fillers.

## Acknowledgment

This research is funded by the Hanoi University of Science and Technology (HUST) under project number T2022-PC-017.

## References

[1] F.-L. Guan *et al.*, "Enhanced thermal conductivity and satisfactory flame retardancy of epoxy/alumina composites by combination with graphene nanoplatelets and magnesium hydroxide," Composites Part B: Engineering, vol. 98, pp. 134-140, Aug. 2016.

[2] J. Li *et al.*, "An Electromechanical Model and Simulation for Test Process of the Wafer Probe," IEEE Transactions on Industrial Electronics, vol. 64, no. 2, pp. 1284-1291, Oct. 2017.

[3] K. Ruan, X. Shi, Y. Guo, and J. Gu, "Interfacial thermal resistance in thermally conductive polymer composites: a review," Composites Communications, vol. 22, p. 100518, Dec. 2020.

[4] I. H. Tavman, *In Nanoengineered Nanofibrous Materials*. Dordrecht, Netherlands: NATO Science Series II, Mathematics, Physics and Chemistry, 2004, p. 449.

[5] C. Xiao, H. He, J. Li, S. Cao, and W. Zhu, "An effective and efficient numerical method for thermal management in 3D stacked integrated circuits," Applied Thermal Engineering, vol. 121, pp. 200-209, July 2017.

[6] X. Qian, J. Zhou, and G. Chen, "Phonon-engineered extreme thermal conductivity materials," Nature Materials, vol. 20, no. 9, pp. 1188-1202, Sep. 2021.

[7] L.-C. Jia *et al.*, "Highly thermally conductive liquid metal-based composites with superior thermostability for thermal management," Journal of Materials Chemistry C, vol. 9, no. 8, pp. 2904-2911, 2021.

[8] K. Yu, T. Yuan, S. Zhang, and C. Bao, "Hypergravity-induced accumulation: A new, efficient, and simple strategy to improve the thermal conductivity of boron nitride filled polymer composites," Polymers, vol. 13, no. 3, p. 459, Jan. 2021.

[9] N. Burger *et al.*, "Review of thermal conductivity in composites: Mechanisms, parameters and theory," Progress in Polymer Science vol. 61, pp. 1-28, Oct. 2016.

[10] F. Zhang, Y. Feng, and W. Feng, "Three-dimensional interconnected networks for thermally conductive polymer composites: Design, preparation, properties, and mechanisms," Materials Science Engineering: R: Reports, vol. 142, p. 100580, Oct. 2020.

[11] X. Bai *et al.*, "Recent progress in thermally conductive polymer/boron nitride composites by constructing three-dimensional networks," Composites Communications, vol. 24, p. 100650, Apr. 2021.

[12] J. Wei *et al.*, "Enhanced thermal conductivity of polydimethylsiloxane composites with carbon fiber," Composites Communications, vol. 17, pp. 141-146, Feb. 2020.

[13] S. Stankovich *et al.*, "Graphene-based composite materials," (in English), Nature, vol. 442, no. 7100, pp. 282-286, July 2006.

[14] I. H. Tavman, "Thermal and mechanical properties of copper powder filled poly (ethylene) composites," Powder Technology, vol. 91, no. 1, pp. 63-67, Apr. 1997.

[15] C.-P. Feng *et al.*, "Electrically insulating, layer structured SiR/GNPs/BN thermal management materials with enhanced thermal conductivity and breakdown voltage," Composites Science Technology, vol. 167, pp. 456-462, Oct. 2018.

[16] X. J. Zha *et al.*, "Enhanced thermal conductivity and balanced mechanical performance of PP/BN composites with 1 vol% finely dispersed MWCNTs assisted by OBC," Advanced Materials Interfaces, vol. 6, no. 9, p. 1900081, May 2019.

[17] W. Si *et al.*, "Enhancing thermal conductivity via conductive network conversion from high to low thermal dissipation in polydimethylsiloxane composites," Journal of Materials Chemistry C, vol. 8, no. 10, pp. 3463-3475, 2020.

[18] Q. H. Mu, S. Y. Feng, and G. Z. Diao, "Thermal conductivity of silicone rubber filled with ZnO," (in English), Polymer Composites, vol. 28, no. 2, pp. 125-130, Apr. 2007.

[19] S. Z. Yu, P. Hing, and X. Hu, "Thermal conductivity of polystyrene-aluminum nitride composite," (in English), Composites Part a-Applied Science and Manufacturing, vol. 33, no. 2, pp. 289-292, Feb. 2002.

[20] H. S. Tekce, D. Kumlutas, and I. H. Tavman, "Effect of particle shape on thermal conductivity of copper reinforced polymer composites," (in English), Journal of Reinforced Plastics and Composites, vol. 26, no. 1, pp. 113-121, Jan. 2007.

[21] M. K. Hassanzadeh-Aghdam and M. J. Mahmoodi, "Micromechanical modeling of thermal conducting behavior of general carbon nanotube-polymer nanocomposites," Materials Science and Engineering: B, vol. 229, pp. 173-183, Mar. 2018.

[22] M. K. Hassanzadeh-Aghdam, R. Ansari, M. J. Mahmoodi, A. Darvizeh, and A. Hajati-Modaraei, "A comprehensive study on thermal conductivities of wavy carbon nanotube-reinforced cementitious nanocomposites," Cement and Concrete Composites, vol. 90, pp. 108-118, July 2018.

[23] M. K. Hassanzadeh-Aghdam and R. Ansari, "Thermal conductivity of shape memory polymer nanocomposites containing carbon nanotubes: A micromechanical approach," Composites Part B: Engineering, vol. 162, pp. 167-177, Apr 2014.

[24] Z. Liu, J. Li, C. Zhou, and W. Zhu, "A molecular dynamics study on thermal and rheological properties of BNNS-epoxy nanocomposites," International Journal of Heat and Mass Transfer, vol. 126, pp. 353-362, Nov. 2018.

[25] Y. C. Zhou *et al.*, "Enhanced high thermal conductivity and low permittivity of polyimide based composites by core-shell Ag@SiO2 nanoparticle fillers," (in English), Applied Physics Letters, vol. 101, no. 1, pp. 0129031-0129034, July 2012.

[26] I.-L. Ngo and C. Byon, "An extensive study on enhancing the thermal conductivity of core–shell nanoparticle composites using finite element method," International Journal of Heat and Mass Transfer, vol. 101, pp. 147-155, Oct. 2016.

[27] I.-L. Ngo, S. V. Prabhakar Vattiktui, and C. Byon, "Effects of thermal contact resistance on the thermal conductivity of core-shell nanoparticle polymer composites," International Journal of Heat and Mass Transfer, vol. 102, pp. 713-722, Nov. 2016.

[28] J. A. King, R. L. Barton, R. A. Hauser, and J. M. Keith, "Synergistic effects of carbon fillers in electrically and thermally conductive liquid crystal polymer based resins," (in English), Polymer Composites, vol. 29, no. 4, pp. 421-428, Apr. 2008.

[29] I.-L. Ngo and C. Byon, "A generalized correlation for predicting the thermal conductivity of composites with heterogeneous nanofillers," International Journal of Heat and Mass Transfer, vol. 90, no. November, pp. 894-899, Nov. 2015.

[30] I. L. Ngo and V. A. Truong, "An investigation on effective thermal conductivity of hybrid-filler polymer composites under effects of random particle distribution, particle size and thermal contact resistance," International Journal of Heat and Mass Transfer, vol. 144, p. 118605, Dec. 2019.

[31] K. Sanada, Y. Tada, and Y. Shindo, "Thermal conductivity of polymer composites with close-packed structure of nano and micro fillers," (in English), Composites Part a-Applied Science and Manufacturing, vol. 40, no. 6-7, pp. 724-730, July 2009.

[32] K. B. Nilagiri Balasubramanian and T. Ramesh, "Role, effect, and influences of micro and nano- fillers on various properties of polymer matrix composites for microelectronics: a review," Polymers for Advanced Technologies, vol. 29, no. 6, pp. 1568-1585, June 2018.

[33] Z. Gao and L. Zhao, "Effect of nano-fillers on the thermal conductivity of epoxy composites with micro-Al2O3 particles," Materials & Design, vol. 66, pp. 176-182, Feb. 2015.

[34] I. L. Ngo, C. Byon, and B. J. Lee, "Numerical analysis for the effects of particle distribution and particle size on effective thermal conductivity of hybrid-filler polymer composites," International Journal of Thermal Sciences, vol. 142, pp. 42-53, 2019.

[35] C.-W. Nan, R. Birringer, D. R. Clarke, and H. Gleiter, "Effective thermal conductivity of particulate composites with interfacial thermal resistance," Journal of Applied Physics, vol. 81, no. 10, pp. 6692-6699, May 1997.

[36] Z. Hashin and S. Shtrikman, "A Variational Approach to the Theory of the Effective Magnetic Permeability of Multiphase Materials," Journal of Applied Physics, vol. 33, no. 10, pp. 3125-3131, Oct. 1962.

[37] Z. Hashin, "Assessment of the Self Consistent Scheme Approximation: Conductivity of Particulate Composites," Journal of Composite Materials, vol. 2, no. 3, pp. 284-300, July 1968.

[38] I.-L. Ngo, S. V. Prabhakar Vattikuti, and C. Byon, "A modified Hashin-Shtrikman model for predicting the thermal conductivity of polymer composites reinforced with randomly distributed hybrid fillers," International Journal of Heat and Mass Transfer, vol. 114, pp. 727-734, Nov. 2017.

[39] I.-L. Ngo and C. Byon, "A generalized correlation for predicting the thermal conductivity of composite materials," International Journal of Heat and Mass Transfer, vol. 83, no. April, pp. 408-415, Apr. 2015.

[40] R. C. Progelhof, J. L. Throne, and R. R. Ruetsch, "Methods for predicting the thermal conductivity of composite systems: A review," Polymer Engineering & Science, vol. 16, no. 9, pp. 615-625, Sep. 1976.

[41] H. Chen *et al.*, "Thermal conductivity of polymer-based composites: Fundamentals and applications," Progress in Polymer Science, vol. 59, pp. 41-85, Aug. 2016.